Electron-spin relaxation and molecular dynamics in liquids. II. Density dependence[a)]

Stephen A. Zager and Jack H. Freed

Baker Laboratory of Chemistry, Cornell University, Ithaca, New York 14853
(Received 26 March 1982; accepted 4 June 1982)

A pressure-dependent ESR relaxation study of the probe PD-tempone dissolved in toluene-$d8$ is described. Extensive results on rotational relaxation, in which $\tau_R(T,P)$ is varied over more than two orders of magnitude, are presented. These results are found to be inconsistent with a simple Stokes–Einstein type η/T behavior modified with a nonzero intercept. However, the data were successfully fit by the empirical form $\tau_R = c\eta\beta(\rho - \tilde{\rho})/T$, where β is the isothermal compressibility, c is a constant, and $\tilde{\rho}$ is an (empirical) reference density whose inverse can be thought of as an "expanded volume". Thus, $\rho - \tilde{\rho}$ is a measure of the strength of the anisotropic intermolecular interactions acting on the probe, while β^{-1} may be thought of as a measure of the total intermolecular interactions. These results for a solute of molecular size somewhat greater than that of the solvent molecules exhibit some differences when compared to a previous NMR study on neat toluene-$d8$. The ϵ parameter introduced by Freed and co-workers to fit their nonsecular spectral densities is found to be independent of temperature and pressure, and it is pointed out that this could be consistent with an intermolecular fluctuating torque model.

I. INTRODUCTION

In I[1] we studied the reorientational dynamics of the probe PD-Tempone in a variety of solvents. In this work we describe an ESR study of PD-Tempone in one solvent, toulene-$d8$, as a function of both temperature and pressure. In this way we can examine in a systematic manner the (possible) dependence of molecular reorientation in liquids on the various thermodynamic and transport properties of the liquid that are also functions of temperature and pressure. In particular, there is considerable interest in the validity of a Stokes–Einstein model whereby the rotational correlation time would be given by

$$\tau_R = \frac{4}{3}\pi\frac{r_e^3\eta}{kT} \equiv \frac{v\eta}{kT} , \tag{1}$$

or else some modification of it. Some of the numerous studies, as well as modifications of Eq. (1) that have been introduced to explain them, are summarized in recent reviews.[2–4] These include both hydrodynamic and molecular models and combinations of them. In general, in comparing with such models, it is useful to analyze the experimental results as a function of temperature and specific volume (or density) especially when relating to free-volume[3] types of theories or to microscopic theories, the object being to furnish an experimental basis for a molecular theory of motional dynamics in liquids.[5,6] This is an objective of the present work. The evidence given in I was consistent with Eq. (1) provided only r_e, the effective rotational radius is adjusted for each solvent. We find in this study that our extensive results as a function of T and P are *inconsistent* with Eq. (1). We are empirically able to establish a new modified form which correlates well with all our data on the PD-Tempone-toulene-$d8$ system covering more than two orders of magnitude variation in τ_R.

We also examine the range of validity of a modification of the Debye spectral density $j(\omega)$ given by

$$j(\omega_0) = \frac{\tau_R}{1 + \epsilon\omega_0^2\tau_R^2} , \tag{2}$$

where ϵ is a correction factor introduced by Freed and co-workers[7,8] in the interpretation of ESR studies of molecular probes in a variety of solvents, and ω_0 is the electron-spin Larmor frequency. It was found, in I generally to be a constant for each solvent, i.e., independent of temperature. The question remains whether ϵ will also prove to be independent of pressure, i.e., can we write $j(\omega)$ as a function of T and P only via its dependence on τ_R. In this way we might be more confident of the origin of ϵ in the molecular reorientational dynamics as opposed to, e.g., some intramolecular process. Jonas[9] has previously pointed out the value of pressure-dependent studies in distinguishing intramolecular from intermolecular dynamical processes. The theoretical models utilized in I to interpret ϵ are based on generalized molecular models for the reorientation process.

There has been a number of pressure-dependent NMR studies of molecular dynamics (a number of which are reviewed by Jonas[9]) but only a few ESR studies[10,11] presumably because of the greater difficulty of the latter. Nevertheless, we believe the present study further demonstrates their usefulness. In our choice of solvent we are able to take advantage of the detailed study[8] of PD-Tempone in toluene-$d8$ as well as the extensive pressure measurements on toluene-$d8$ by Wilbur and Jonas.[12]

II. EXPERIMENTAL DESCRIPTION

The experiments were performed as isothermal variable pressure runs. Although no hysteresis was observed in pressurization, measurements were always made with ascending pressure. A schematic diagram of the equipment used for this work is given in Fig. 1. The high pressure ESR vessel has been described previously,[11] and the operation of the high pressure gen-

[a)]Supported by NSF Grant No. CHE 8024124.

 0021-9606/82/193360-16$02.10

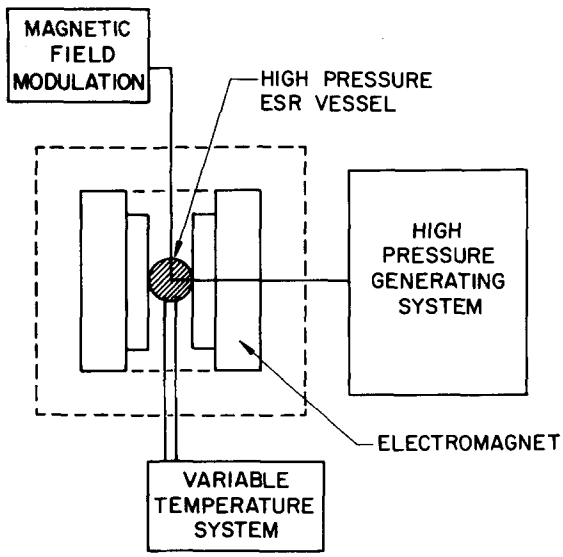

FIG. 1. Schematic diagram of the high pressure ESR equipment.

erating equipment is described elsewhere.[13] New features of the high pressure vessel as well as descriptions of the more difficult problems encountered in its use are also given there.[13]

Variable temperature control was effected by circulating a thermostated liquid through copper coils fixed in a cylindrical stainless steel jacket that encloses the high pressure vessel. The 350 ml volume between the copper coils and the high pressure vessel was filled with heat transfer fluid to promote rapid, uniform temperature equilibration. The jacket temperature was monitored with a copper–Constantan thermocouple. For temperatures below $-20\,^{\circ}C$ we used a Neslab Cyrotrol temperature controller in conjunction with a Neslab *U*-Tainer *B* insulated bath, Cryoflow *B* agitator and circulator, and CryoCool CC-80II immersion cooler. The low temperature heat transfer fluid was 90%, 95% ethanol and 10% acetone. The refrigeration equipment is capable of taking an unstirred Dewar of this fluid to $-80\,^{\circ}C$, but the thermal load presented by the thinly insulated high pressure vessel increases the minimum working temperature to $-39\,^{\circ}C$. Temperatures above $-10\,^{\circ}C$ were produced by a Neslab Tamson TEV45 thermostatic bath and circulator run against a PBC-2 bath cooler. For this system the heat transfer fluid was a mixture of automotive antifreeze and water.

All spectra were recorded at X band with a Varian E-12 spectrometer using 10 kHz field modulation. The magnetic field modulation and microwave power were continually adjusted to avoid line shape distortion. The high pressure ESR vessel is mounted on standard X-band waveguide and replaces the conventional microwave cavity in the region between the electromagnet pole pieces. A thorough description of the microwave helix system is given by Plachy.[14] A wooden frame holds the assembled vessel permitting easy and reproducible centering of the sample in the magnetic field region. This frame also provides a stable base for the vessel, serves as an additional layer of thermal insulation, and offers some protection in the event of a serious high pressure failure.

Spectrometer operation was modified in several ways. A broad dip in the klystron power mode was located by changing the klystron frequency. The resonant structure consisting of the hybrid coaxial-helical transmission line was then matched to the rest of the microwave circuit with a sliding short. To compensate for out-of-phase signals due to reflections introduced by the microwave transmission line, it was necessary to switch off the klystron AFC circuit. Then fine adjustment of the phase control on the reference arm was used to symmetrize the ESR line shape. In this way we were generally able to maintain lineshape symmetries better than 95%. It was also sometimes helpful to use less than optimal coupling to effect symmetrization. Microwave frequency drift was minimized by sufficient klystron warmup. Frequency measurements were routinely made with a Systron Donner 1037 counter before and after each data set, and frequency changes were typically less than 30 Hz.

PD-Tempone was synthesized as in I and care was taken in its handling to minimize air contact. Toluene-*d*8 (99.5% D, Stohler Isotope Chemicals,) was distilled under vacuum from a sodium mirror and sealed in glass. Solutions of 2×10^{-4} M PD-Tempone in toluene-*d*8 were prepared and loaded into high pressure sample holders under nitrogen as described elsewhere,[12] where the subsequent deoxygenation method is also described.

The experiments were performed with liquid samples. Toluene readily supercools with increased pressure, as it does with decreased temperature.[15] Evidence for this comes from the fact that although our two lowest temperature runs crossed the liquid–solid coexistence curve in the phase diagram of toluene,[16] we did not observe a rigid limit ESR spectrum under these conditions. The extent of supercooling is considerable. At $-39.2\,^{\circ}C$, freezing had not yet occurred 1.2 kbar above the melting point of 3.3 kbar, and in preliminary work at $-78\,^{\circ}C$ freezing was finally found 4.5 kbar beyond the melting point of 0.6 kbar. Thus, the high viscosity region of liquid toluene is conveniently studied as a function of pressure.

No significant temperature dependence[8] nor pressure dependence was observed for a_N and a_D.

We list in Table I the relevant physical properties of toluene-*d*8 (viz., density and viscosity). The small amount of solute was assumed to have negligible effect on the pure solvent properties. High pressure density ρ measurements[12] were interpolated and extrapolated according to

$$1/\rho = aT + b \quad \text{(at constant pressure)}, \tag{3a}$$

and

$$1/\rho = c \ln P + d \quad \text{(at constant temperature)}. \tag{3b}$$

High pressure viscosity η data[12] were interpolated and extrapolated according to

$$\ln \eta = a/T + b \quad \text{(at constant pressure)}, \tag{4a}$$

and

TABLE I. Linewidth results for PD-Tempone in toluene-$d8$ and physical properties.

T °C	P(kbar)	ρ(g/cm^3)[b]	η(cP)[b]	A(mG)	B(mG)	C(mG)	τ_R(s)
51.59±0.02	0.001	0.909	0.454	263.1	5.41	3.21	3.4×10^{-12} [a]
51.59±0.02	0.513	0.947	0.640	212.6	6.84	3.81	4.5×10^{-12} [a]
51.59±0.02	1.011	0.977	0.853	187.4	7.53	4.81	5.1×10^{-12} [a]
51.59±0.02	1.517	1.000	1.10	165.6	9.38	5.41	6.8×10^{-12} [a]
51.59±0.02	2.020	1.019	1.39	153.0	9.87	6.61	7.3×10^{-12} [a]
51.59±0.02	2.525	1.038	1.76	137.1	11.69	7.15	9.2×10^{-12} [a]
25.11±0.03	0.001	0.934	0.607	212.3	7.40	3.96	5.0×10^{-12}
25.11±0.03	0.510	0.969	0.847	174.9	9.37	5.28	6.7×10^{-12}
25.11±0.03	1.043	0.997	1.16	153.4	10.95	6.30	8.0×10^{-12}
25.11±0.03	1.515	1.018	1.49	134.3	12.50	8.03	9.8×10^{-12}
25.11±0.03	2.030	1.036	1.95	127.8	15.69	10.81	1.3×10^{-11}
25.11±0.03	2.520	1.055	2.41	107.7	19.0	15.1	1.73×10^{-11}
25.11±0.03	3.027	1.072	3.09	109.9	22.55	17.52	2.06×10^{-11}
25.11±0.03	3.518	1.089	3.95	105.6	26.46	21.78	2.5×10^{-11}
25.11±0.03	4.022	1.101	5.08	99.1	30.62	27.25	3.02×10^{-11}
25.11±0.03	4.520	1.113	6.47	102.1	37.15	34.01	3.73×10^{-11}
1.8±0.1	0.001	0.957	0.866	163.2	10.08	6.25	7.6×10^{-12}
1.8±0.1	0.527	0.990	1.19	133.4	12.96	9.1	1.07×10^{-11}
1.8±0.1	1.060	1.015	1.65	113.2	16.48	11.66	1.4×10^{-11}
1.8±0.1	1.525	1.035	2.24	101.4	18.56	15.64	1.75×10^{-11}
1.8±0.1	2.001	1.052	2.93	97.1	23.06	18.97	2.15×10^{-11}
1.8±0.1	2.518	1.070	3.97	94.1	29.96	26.28	2.9×10^{-11}
1.8±0.1	2.989	1.087	5.20	98.2	36.03	32.8	3.62×10^{-11}
1.8±0.1	3.383	1.107	6.54	103.1	44.6	41.2	4.54×10^{-11}
1.8±0.1	4.027	1.121	9.51	124.9	63.0	60.8	6.57×10^{-11}
1.8±0.1	4.538	1.135	12.8	147.8	81.5	78.6	8.5×10^{-11}
1.8±0.1	5.049	1.148	17.2	185.2	112.9	110.2	1.19×10^{-10}
1.8±0.1	5.46	1.160	21.8	225.2	143.2	137.0	1.5×10^{-10}
−24.1±0.3	0.001	0.984	1.39	113.2	15.39	10.86	1.3×10^{-11}
−24.1±0.3	0.528	1.015	1.83	98.8	20.53	15.59	1.85×10^{-11}
−24.1±0.3	1.015	1.035	2.54	92.4	27.15	22.69	2.6×10^{-11}
−24.1±0.3	1.520	1.054	3.83	91.6	33.92	30.00	3.4×10^{-11}
−24.1±0.3	2.023	1.070	5.22	98.0	45.6	42.0	4.65×10^{-11}
−24.1±0.3	2.520	1.087	7.74	111.4	56.9	56.6	6.25×10^{-11}
−24.1±0.3	3.024	1.104	10.9	138.8	82.8	78.3	8.6×10^{-11}
−24.1±0.3	3.521	1.127	15.4	178.6	112.8	109.6	1.2×10^{-10}
−24.1±0.3	4.041	1.142	22.0	247.1	163.2	157.4	1.7×10^{-10}
−24.1±0.3	4.533	1.157	31.0	352.9	233.6	226.9	2.45×10^{-10}
−39.2±0.3	0.001	1.001	1.92	118.9	22.01	17.84	2.05×10^{-11}
−39.2±0.3	0.519	1.029	2.46	113.0	30.10	26.55	2.95×10^{-11}
−39.2±0.3	1.023	1.048	3.50	112.9	41.28	37.29	4.13×10^{-11}
−39.2±0.3	1.520	1.065	5.54	129.5	57.51	53.47	5.85×10^{-11}
−39.2±0.3	2.031	1.080	7.74	148.4	78.2	73.4	8.03×10^{-11}
−39.2±0.3	2.523	1.098	12.2	215.7	119.0	111.3	1.22×10^{-10}
−39.2±0.3	3.035	1.114	18.0	310.8	179.6	174.0	1.91×10^{-10}
−39.2±0.3	3.523	1.138	26.3	436.6	274.9	266.3	2.92×10^{-10}
−39.2±0.3	4.027	1.155	38.4	658.9	403.6	384.3	4.23×10^{-10}
−39.2±0.3	4.529	1.171	56.8	1043.1	609.0	589.6	6.54×10^{-10}

[a]Determined from linewidth coefficient B.

[b]From Ref. 12.

$$\ln\eta = cP + d \quad \text{(at constant temperature)} . \tag{4b}$$

Measurements of the density[17] and viscosity[15,18] of toluene-$h8$ were used to check Eqs. (3) and (4). To account for perdeuteration, a simple correction to these properties has been given.[19,20]

III. RESULTS AND ANALYSIS

A. Linewidths and relaxation times: The ϵ parameter

Linewidth and hyperfine splitting data were collected on line and processed in a Prime 400 computer.[13] The room temperature, atmospheric pressure linewidth was checked before each run to check on the sample, and the atmospheric pressure linewidth at the day's working temperature was always found to be unchanged after the pressurization.

The ESR spectra were in the motionally narrowed regime. Details of the treatment of the linewidth data are given elsewhere.[13] The resulting linewidth coefficients A, B, and C are given in Table I. Each temperature given is an average obtained over the course of an isothermal experiment; the uncertainties reflect the entire observed range. A set of measurements at one pressure required about 30 min, and during that time

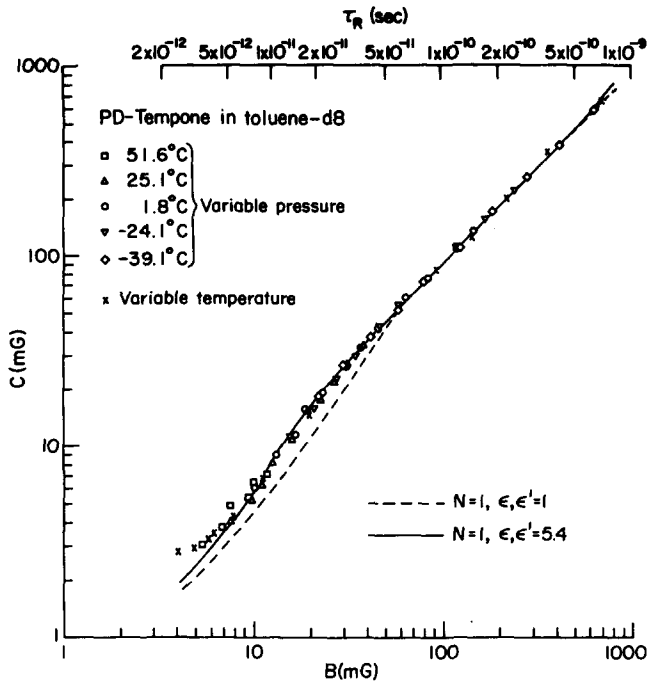

FIG. 2. A comparison of experimental and calculated values of C vs B for PD-Tempone in tuluene-$d8$. Variable pressure and temperature results.

the pressure was recorded at 5 min intervals. These results were combined to determine the mean pressures shown; typical standard deviations were less than 0.0002 kbar.

The parameters that are obtained from the experimental analysis are $\tau_{\bar{R}}$, N, ϵ, and ϵ'. They are based upon a model of axially symmetric rotational diffusion with $R_{\parallel}$ and $R_{\perp}$ the components of the rotational diffusion tensor parallel and perpendicular to the main symmetry axis. Then the mean rotational correlation time $\tau_{\bar{R}} \equiv (6R_{\parallel}R_{\perp})^{-1}$ and the rotational anisotropy parameter $N \equiv R_{\parallel}/R_{\perp}$, so in the limit of isotropic rotation $N=1$ and we let $\tau_{\bar{R}} = \tau_R$. We use ϵ as the correction to the nonsecular spectral density as given in Eq. (2), while ϵ' is the similarly defined term to correct $j(\omega_n)$, where ω_n is of the order of the hyperfine frequency. These parameters are obtained as follows: First, for each isotherm, the experimental values of the linewidth parameters C were plotted versus those of B. Then, using the theoretical expressions for B and C[7] and the magnetic tensors for PD-Tempone in toluene-$d8$, theoretical curves of $C = C(\tau_{\bar{R}})$ vs $B = B(\tau_{\bar{R}})$ are drawn for different sets of the dimensionless parameters N, ϵ, and ϵ'. The curve that best passes through the data points yields the best estimate of N, ϵ, and ϵ'. These curves were used to establish the τ_R values given in Table I.

Several conclusions follow from examination of the variable pressure results. First, for each isotherm the best choice of N, ϵ, and ϵ' yields a curve that fits the experimental points very well. This establishes confidence in both the theoretical analysis and the quality of the high pressure data. Second, the *same* set of values, $N=1$, $\epsilon = \epsilon' = 5.4$ was independently obtained from each of the isotherms, indicating that the molecular reorientation process has the same characteristics under all the conditions studied. Third, the description of the rotational diffusion that emerges is then simply dependent only on $\tau_{\bar{R}} = \tau_R$, independent of the parametric dependence of τ_R on pressure and temperature [i.e., $\tau_R = \tau_R(T, P)$]. These three points are best illustrated by Fig. 2 which combines all the variable pressure and variable temperature data for PD-Tempone to toluene-$d8$.

Some qualification of the preceeding remarks is appropriate. The limited range of τ_R covered by each isotherm does not really permit careful fitting of all three parameters N, ϵ, and ϵ' for each isotherm. Thus, for example, it can be seen in Fig. 2 that ϵ' affects the results for $\tau_R \geq 4\times10^{-10}$ s, a region accessible to only the $-39.2\,^{\circ}$C isotherm. However, the fact that the individual isotherms overlap and join together smoothly is consistent with the stated conclusions.

We thus find that Eq. (2) with constant ϵ is a very good representation of the results for PD-Tempone in toluene-$d8$. The temperature and pressure independence of ϵ appear to be best fit by the fluctuating torque model as discussed in I. That is, in the fluctuating torque model[1] $\epsilon \approx (1+\tau_M/\tau_R)^{1/2}$, where τ_M is the relaxation time of the torques, and where $\tau_R = \tau_M\,(IV^2/6k_BT)$ with $(Ik_BT)V^2$ the mean-square value of the fluctuating torques and I the moment of inertia. If we regard τ_M as an activated state process such as is τ_R [cf. Eq. (5) below], then the constancy in ϵ (within our experimental uncertainties) would imply very nearly the same activation law for both τ_R and τ_M as is required by the above relation for τ_R in terms of τ_M (to within the much weaker T and P variation of the mean-square value of the fluctuating torques, which should just affect preexponential factors in an activated state analysis). Other intermolecular models discussed in I (e.g., SRLS) would not be expected to yield a constant ϵ.[1] It is difficult to rationalize our simple result in terms of an explanation for ϵ involving contributions from an intramolecular (or internal motional) process which typically has a different dependence on T and ρ than the overall reorientational process.[9]

Also the result $N=1$ shows that the reorientation is isotropic and independent of temperature and pressure.

B. Activated state analysis of τ_R

We first summarize our results on τ_R in the familiar activated state formulation[1,11,21,22]

$$\tau_R = \tau_R^0 \exp\left(\frac{\Delta G_a}{RT}\right), \tag{5}$$

where ΔG_a is the change in Gibbs free energy between the initial and activated state. We obtain from the P and T dependence of τ_R:

(1) ΔH_a the enthalpy of activation:

$$\Delta H_a = \left[\frac{\partial(\Delta G_a/T)}{\partial(1/T)}\right]_P = R\left[\frac{\partial \ln \tau_R}{\partial(1/T)}\right]_P . \tag{6}$$

The linear isobars of Fig. 3 lead to the least-squares fit:

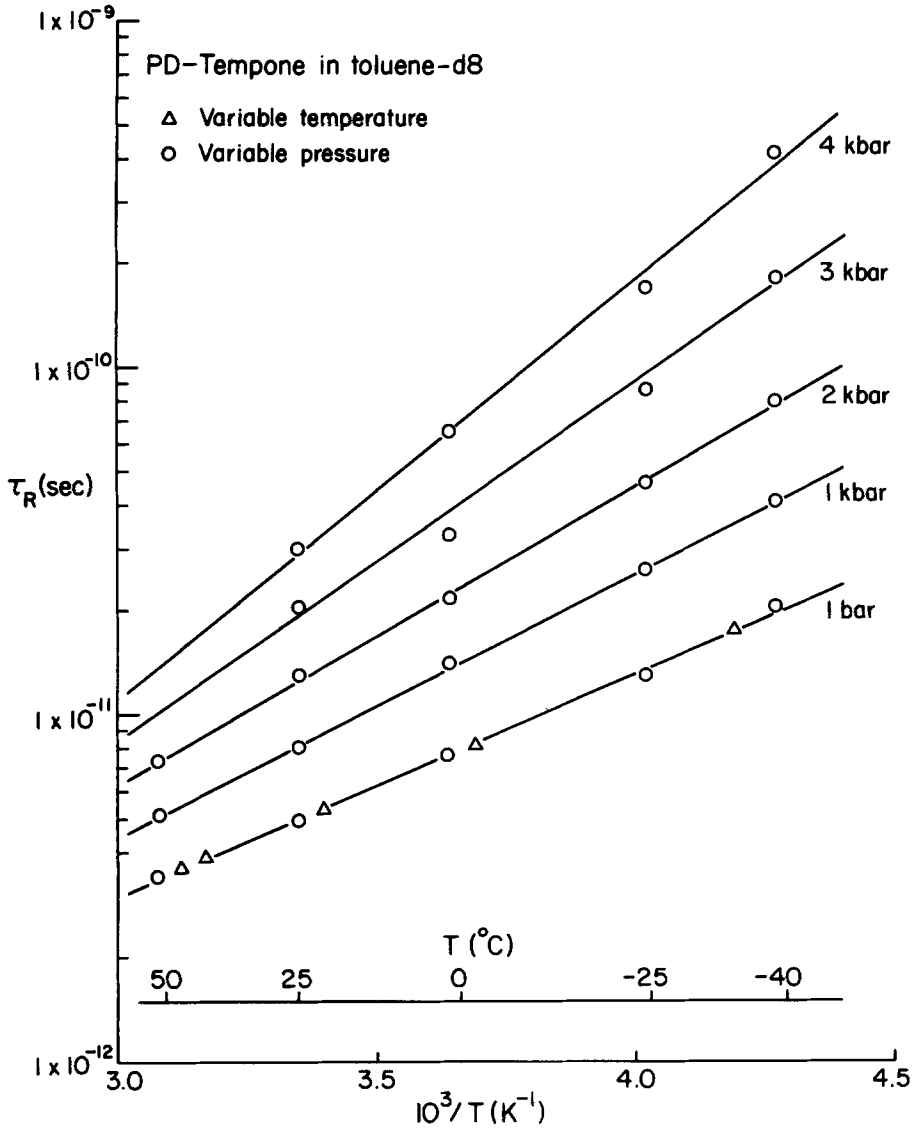

FIG. 3. Isobars of τ_R vs $1/T$ for PD-Tempone in toluene-$d8$. The lines are least-squares fits.

$$\Delta H_a(\text{kcal/mol}) = 2.949 + 0.362\,P(\text{kbar}) + 0.076\,P^2 \ . \tag{7}$$

(2) The volume of activation ΔV_a is

$$\Delta V_a = \left(\frac{\partial \Delta G_a}{\partial P}\right)_T = RT\left(\frac{\partial \ln \tau_R}{\partial P}\right)_T \ , \tag{8}$$

and from the linear isotherms of Fig. 4, the least-squares fit is [cf. Fig. 4(b)]:

$$\Delta V_a(\text{cm}^2/\text{mol}) = 22.39 - 0.0374\ T(\text{K}) \ . \tag{9}$$

(3) The energy of activation ΔE_a is

$$\Delta E_a = \left[\frac{\partial(\Delta G_a/T)}{\partial(1/T)}\right]_\rho = R\left[\frac{\partial \ln \tau_R}{\partial(1/T)}\right]_\rho \tag{10}$$

and from the linear isochores in Fig. 5 we obtain the least-squares result:

$$\Delta E_a(\text{kcal/mol}) = 67.0 - 134.1\rho(\text{gm/cm}^3) + 69.0\rho^2 \tag{11}$$

(which increases monotonically with ρ in the density range studied). An alternative form for ΔE_a is

$$\Delta E_a = \Delta H_a - T(\alpha/\beta)\Delta V_a \ , \tag{12}$$

with α, the coefficient of thermal expansion and β the isothermal compressibility:

$$\alpha = -\rho^{-1}\left(\frac{\partial \rho}{\partial T}\right)_p \ , \tag{13a}$$

$$\beta = \rho^{-1}\left(\frac{\partial \rho}{\partial P}\right)_T \ . \tag{13b}$$

Both α and β can be calculated from the data of Table I, so Eq. (12) serves as a check of the self-consistency of the analysis. It is found that ΔE_a calculated from Eq. (12) agrees very well with Eq. (11). These results are consistent with the usual interpretations.[11,22] Thus ΔH_a is expected to increase with pressure, because decreasing the free volume increases the intermolecular restoring torques. For essentially the same reason, ΔE_a increases with increasing density. Also, as the temperature is increased, the average molecular kinetic fluctuations increase, so the ΔV_a that is needed decreases.

A word of caution is in order with regard to the apparently linear sets of curves of Figs. 3–5. At best,

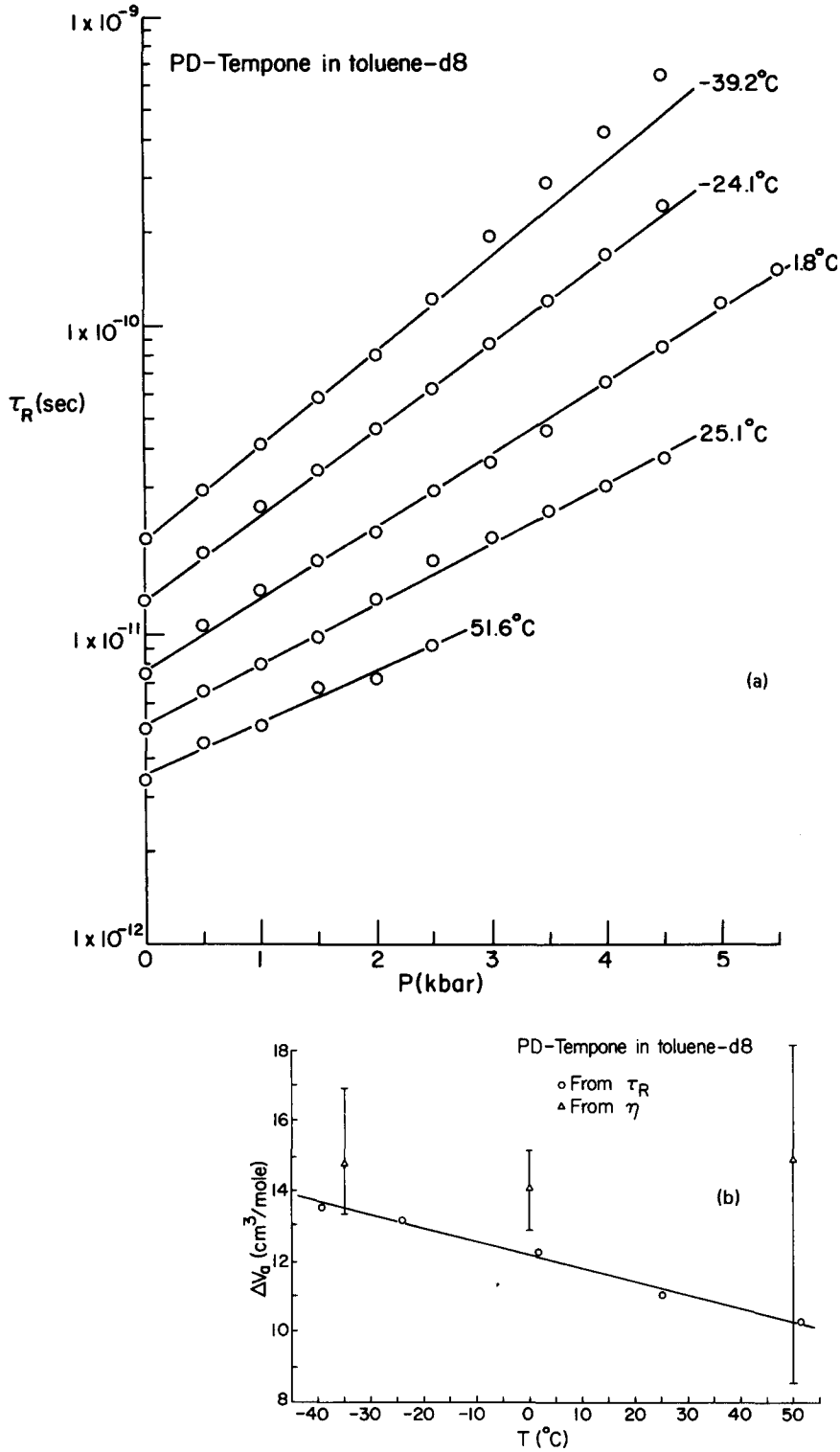

FIG. 4. (a) Isotherms of τ_R vs P for PD-Tempone in toluene-$d8$. The lines are least-squares fit; (b) ΔV_a vs T for PD-Tempone in toluene-$d8$. The line is a least-squares fit to the τ_R data.

a given curve covers a variation in τ_R of one order of magnitude. This is the case for the isobar at 1 atm in Fig. 3. In I the full set of results at 1 atm covering nearly three orders of magnitude in τ_R do show some curvature with $1/T$ and this required an empirical $\Delta H_a = \Delta H_a(1/T)$.

The results of the above analysis for the τ_R of PD-Tempone in toluene-$d8$ are found to parallel those obtained for the overall molecular reorientation in neat toluene-$d8$ obtained by Wilbur and Jonas,[12] but to show significant differences as we discuss in Sec. III E.[23]

We show in Fig. 4(b) results of Wilbur and Jonas[12] for the volume of activation ΔV_a for the viscosity of toluene-$d8$. The large error bars we show are because we find that the isotherms of $\ln\eta$ vs P are not linear; (the nonlinearity becomes more significant for the lower pressures at higher temperatures). Instead of a pressure dependent ΔV_a^{η}, the error bars indicate the range

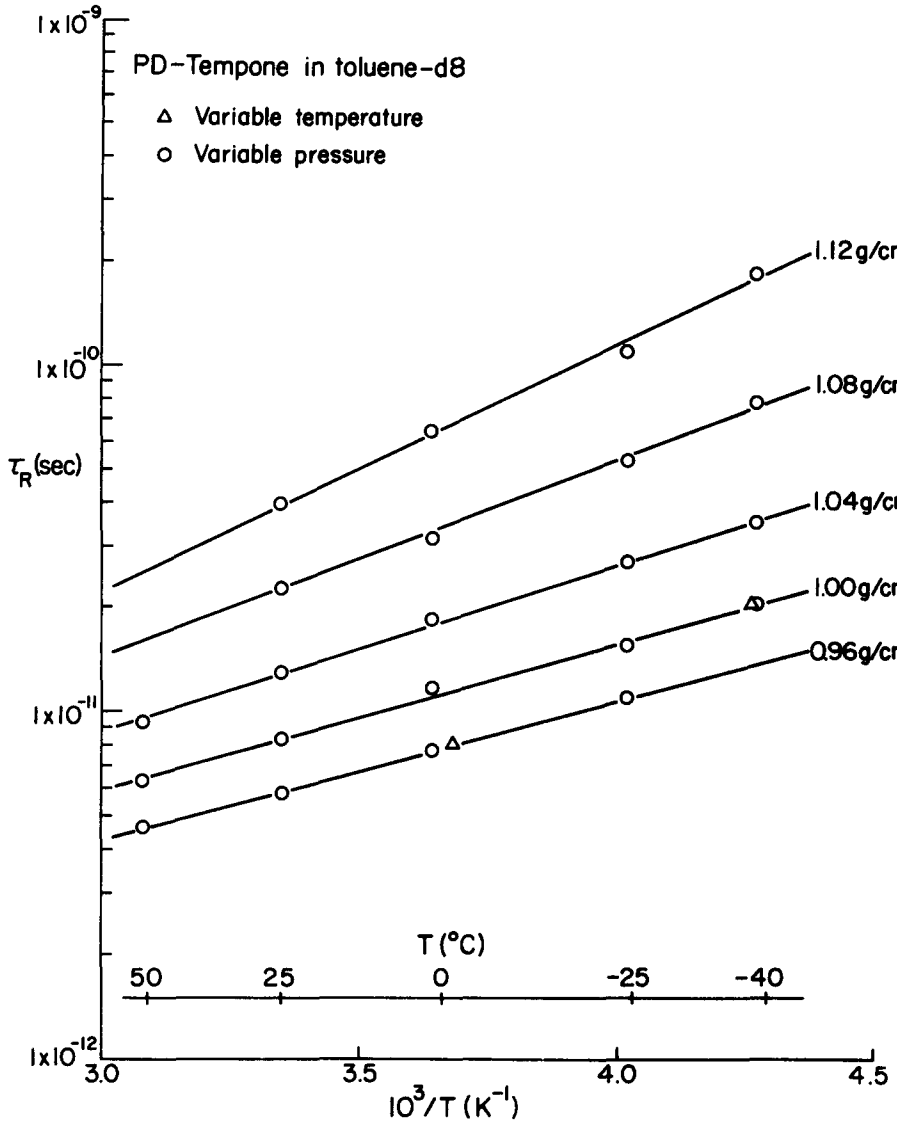

FIG. 5. Isochores of τ_R vs $1/T$ for PD-Tempone in toluene-$d8$. The lines are least-squares fits.

of values obtained from simple differentiation of the viscosity isotherms. Discussion of these matters is deferred to Sec. III E.

C. Stokes-Einstein forms

In general, we found in I that a Stokes–Einstein type of behavior [Eq. (1)] provided a good description of the results of PD-Tempone in a variety of solvents. In particular, the data were fit to the form

$$\tau_R = A\eta/T + \tau_R^0 , \tag{14}$$

and A was found to depend only on solvent, while τ_R^0 was found, for the most part, to be zero within experimental error. The form of Eq. (14) was originally introduced to account for orientational relaxation times measured by depolarized Rayleigh scattering.[24] This work was performed close to room temperature and atmospheric pressure; the solution viscosity was varied by mixing the optically anisotropic probe molecule with different amounts of optically isotropic solvents. In this way several molecular liquids, including toluene, were studied over the limited viscosity range of 0.2–2 cP.[25] Room temperature depolarized Rayleigh scattering of toluene under high pressure has since been performed.[26] Variable temperature ESR experiments on a variety of spin probes and solvents have also addressed this matter.[27] Equation (14) with a temperature-dependent slope $C(T)$ and intercept $\tau_R^0(T)$ was used to analyze reorientational correlation times obtained using pressure to change the viscosity of nine neat liquids.[28]

We now consider our results in the light of Eq. (14). Isotherms of τ_R vs η/T obtained by varying pressure are found to be well represented by straight lines. However, the slopes and intercepts of these lines are temperature dependent. The data were fit to Eq. (14) and the least-squares parameters are given in Table II for the isotherms. Both the slope and intercept (which is now non-negligible) increase with decreasing temperature.

Equation (14) can equally well be tested by plotting isobars in which τ_R and η/T are varied by varying T. The results of such least-squares fits to Eq. (14), are

TABLE II. Least-squares results for $\tau_R(P)$ vs $\eta(P)/T$ at constant temperature.

Temperature (° C)	Slope (10^{-7} s K/P)[a]	Intercept (10^{-12} s)[a]
51.5	1.40 ± 0.07	1.6 ± 0.3
25.1	1.73 ± 0.05	1.8 ± 0.5
1.8	1.85 ± 0.01	1.9 ± 0.5
−24.1	1.91 ± 0.02	4 ± 1
−39.2	2.26 ± 0.05	5 ± 1

[a]Uncertainties represent average deviations.

presented in Table III. Although the slope is nearly pressure independent, there is dramatic increase in the magnitude of the *negative* intercept with increasing pressure. *Only the intercept at* 1 *bar is not statistically different from zero.*[29(a)] Using the Stokes–Einstein relation we can determine an effective rotational radius $r_e = 2.0$ A from this result. In a similar manner we can plot τ_R vs η/T as isochores. They were satisfactorily fit to Eq. (14) and the results appear in Table IV.[29(b)] We see from Table IV that the slope is nearly independent of density, but there is a large negative intercept that increases in magnitude with increasing density. This pattern is similar to that observed for constant pressure.

We cannot reconcile the dramatically different results obtained by the different methods of varying η/T (and summarized in Tables II, III, and IV) in terms of any unifying or fundamental value of Eq. (14). We therefore regard these results as demonstrating the *inadequacy* of a Stokes–Einstein type of relation such as Eq. (14). Furthermore, since all our results are in the τ_R range for which inertial effects have negligible effects on the reorientational dynamics (cf. I), we do not believe there is any theoretical justification for introducing a τ_0 to account for inertial effects.[2]

We have, therefore, sought an approach to represent our data effectively and compactly. The most obvious approach to us is to describe the deviations from Stokes–Einstein behavior in terms of a polynomial function of pressure or density, and temperature.

Thus, e.g., we may write:

$$\tau_R T/\eta = a + bP + cp^2 + dT + eT^2 + fPT + \cdots \quad . \tag{15}$$

TABLE III. Least-squares results for $\tau_R(T)$ vs $\eta(T)/T$ at constant pressure.

Pressure (kbar)	Slope (10^{-7} s K/P)[a]	Intercept (10^{-12} s)[a]
0.001	2.47 ± 0.06	−0.2 ± 0.3
0.5	2.89 ± 0.09	−1.6 ± 0.6
1	2.94 ± 0.05	−3.3 ± 0.5
1.5	2.54 ± 0.07	−2.9 ± 0.9
2	2.52 ± 0.05	−4.3 ± 0.9
2.5	2.36 ± 0.09	−4.4 ± 2.5
3	2.6 ± 0.2	−12 ± 7
3.5	2.7 ± 0.2	−21 ± 12
4	2.7 ± 0.2	−30 ± 17
4.5	2.8 ± 0.2	−49 ± 26

[a]Uncertainties represent average deviations.

TABLE IV. Least-squares results for $\tau_R(T)$ vs $\eta(T)/T$ at constant density.

Density (g/cm^3)	Slope (10^{-7} s K/P)[a]	Intercept (10^{-12} s)[a]
0.96	3.06 ± 0.02	−2.28 ± 0.07
0.98	2.8 ± 0.1	−2.0 ± 0.7
1.00	2.97 ± 0.08	−3.6 ± 0.5
1.02	3.32 ± 0.02	−6.9 ± 0.2
1.04	3.3 ± 0.2	−9.6 ± 1.6
1.06	2.7 ± 0.2	−8.0 ± 2.5
1.08	2.5 ± 0.2	−9.4 ± 5.1
1.10	2.3 ± 0.2	−10 ± 7
1.12	2.5 ± 0.1	−24 ± 5
1.14	3.2 ± 0.4	−84 ± 33
1.16	3.2 ± 0.5	−125 ± 66

[a]Uncertainties represent average deviations.

[In relating to other workers[2,3,10,12] we can regard the right-hand side as equal to $v\kappa(T,P)k_B$, where κ is the dimensionless parameter introduced by Kivelson, see below and v is defined in Eq. (1).] We have performed this fitting by using a stepwise linear regression procedure based upon maximum R^2 improvement.[30] Basically, this method determines the subset of variables, chosen from a given full set of variables, that produces the greatest increase in the value of R^2 for models of all possible sizes. For example, Eq. (15) represents a five-variable model. The variables are P, P^2, T, T^2, and TP; the constant term is not included in the variable count. For this case the stepwise regression method will select the best one-variable model, the best two-variable model, and so on, to the best five-variable model, characterizing each model by the appropriate subset of coefficients and estimated uncertainties. From this collection of equations we can then choose one according to Mallow's c_p statistic.[31] In terms of prediction, this statistic establishes a compromise between a function of too few variables that must be forced through the data points and a function of more variables than is justified by the data. The equation obtained in this way retains only the significant variables, and therefore, should be most useful in relating the essential physical content of the data.

These methods were applied to the data for PD-Tempone in toluene-$d8$. Starting from the full model function given by Eq. (15) we find

$$\frac{\tau_R}{(\eta/T)} = (6.07 \pm 0.64)\times 10^{-7} + (2.79 \pm 0.72)\times 10^{-9} P^2 - (2.24 \pm 0.50)\times 10^{-9} T + (3.44 \pm 0.93)\times 10^{-12} T^2 - (9.78 \pm 1.23)\times 10^{-11} PT \quad . \tag{16}$$

with each term in sec K/poise, P in kbar, and T in K. Based on 60 data points, this fit gives $R^2 = 0.90$ and $c_p = 0.82$. The overall effectiveness of Eq. (16) can be seen from a comparison of Figs. 6 and 7. Figure 6 shows τ_R vs $v\eta/k_BT$ with v calculated from the value $r_e = 2.7 \pm 0.1$ Å obtained from the constant term in Eq. (16). Given that Fig. 6 is a log–log plot, it is apparent that there is considerable scatter from a linear relation. In Fig. 7 we show τ_R vs $(v\eta/k_BT)'$, where $(v\eta/k_BT)'$ is the right-hand side of Eq. (16) after mul-

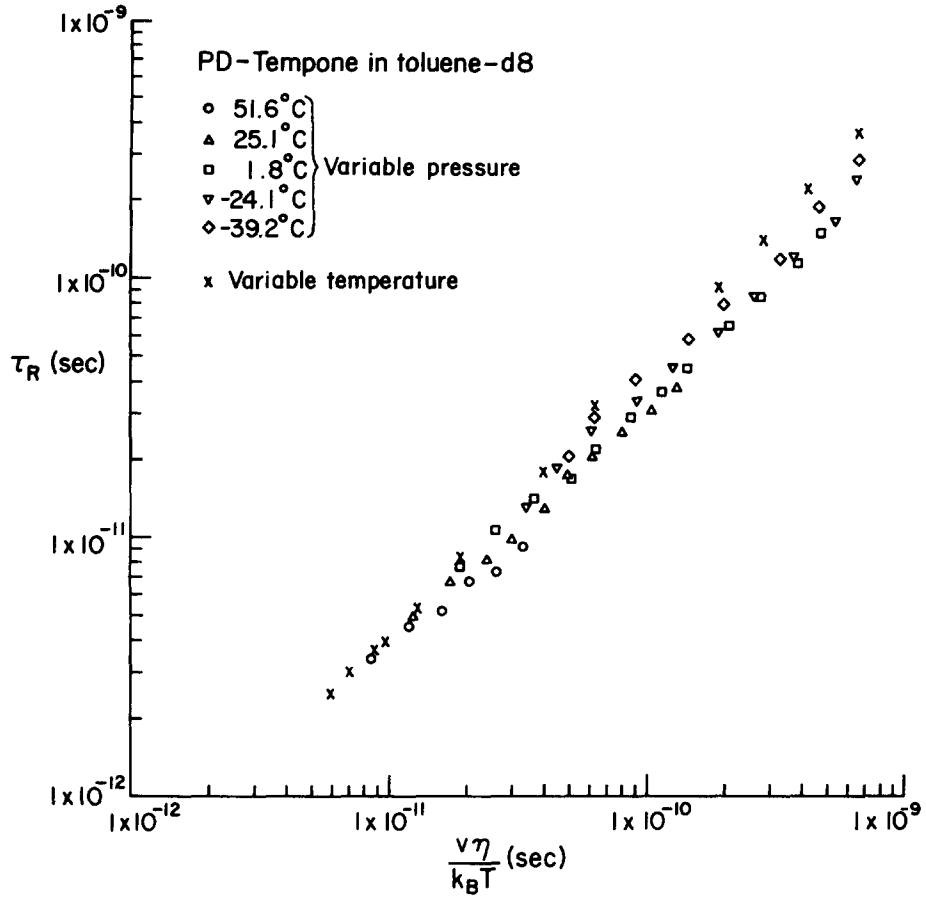

FIG. 6. τ_R vs $v\eta/k_BT$ for PD-Tempone in toluene-$d8$. Variable pressure and temperature results.

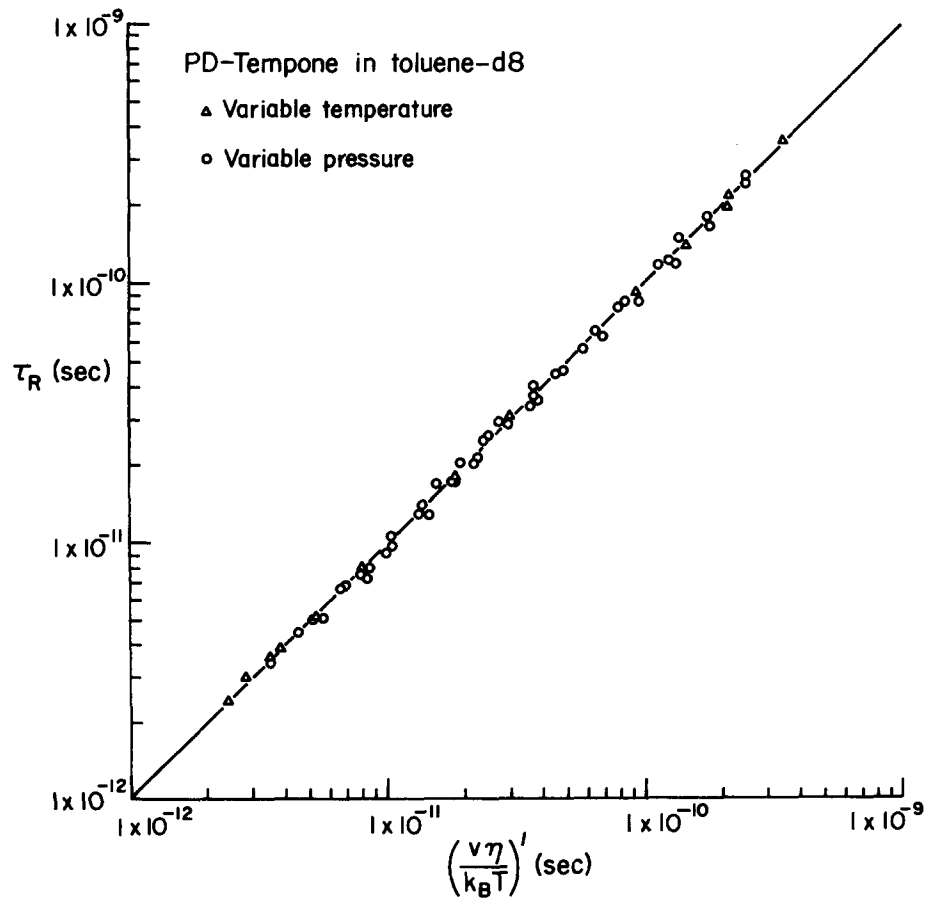

FIG. 7. τ_B vs $(v\eta/k_BT)'$ for PD-Tempone in toluene-$d8$. Variable pressure and temperature results. The identity line is included for comparison.

tiplication by η/T (i.e., $\kappa v\eta/k_BT$, see above). The good straight line fit is maintained over a wide range of pressures and temperatures resulting in a range of τ_R covering more than two orders of magnitude.

We have tested other combinations of variables besides (P, T) in Eq. (15) including (ρ, T), $(1/\rho, T)$, and $(1/\rho, 1/T)$. The resulting R^2 values are not significantly different from that reported for (P, T). For the variables $(1/\rho, T)$, we find

$$\tau_R/(\eta/T) = (5.46 \pm 0.58)\times 10^{-7} - (3.02 \pm 0.40)\times 10^{-9} T + (3.96 \pm 1.7)\times 10^{-12} T^2 + (2.14 \pm 0,17)\times 10^{-7}/\rho^2 , \quad (17)$$

with each term in S-K/P, T in K, and ρ in g/cm^3. With 60 data points, this gives $R^2 = 0.91$ and $c_P = 0.71$ with one less term in the expansion than Eq. (16). This form gives nearly the same value for r_e as that found from Eq. (16). It is our belief that the experimental uncertainties in the data preclude any further improvement in the R^2 test. Equation (17) shows that $\tau_R/(\eta/T)$ always increases with decreasing ρ, and in the temperature range we studied, it decreases with increasing T.

The next task would be to relate these results to some physical model(s). One could proceed using the activated state approach of the previous section to examine the differences between ΔH_a and ΔH_a^η, etc.,[13] and we return to this in Sec. III E. We shall proceed in a different manner here.

Recently Dote *et al.*[3] have proposed a quasihydrodynamic free-space model for molecular reorientation in liquids. When compared to several other models, this one was more successful in correlating a range of experimental results. The theory seeks to explain the factor C (where $v_p = v$) in

$$\tau_R = \frac{v_p \eta}{k_B T} f_{\text{stick}} C + \tau_R^0 , \quad (18)$$

a form entirely analogous to Eq. (14), where f_{stick} is a hydrodynamic coefficient that depends upon the shape of the rotating molecule, and τ_R^0 is taken as zero. (Note that C plays almost the same role as κ defined above.) A measure of the coupling between the rotating molecule and its surroundings, C is written as

$$C = 1/(1 + \gamma/\phi) , \quad (19)$$

where ϕ is a constant that determines the effective rotational volume ϕv_p, and

$$\gamma = B k_B T \beta\eta [4(v_p/v_s)^{2/3} + 1]/v_p . \quad (20)$$

B is the Batchinski constant[3,32,33] that relates free volume to viscosity, β is the isothermal compressibility, and v_s represents the molecular volume of the solvent. In Eq. (20) only the factor $T\beta\eta$ should be significantly pressure and temperature dependent. Thus Eq. (19) becomes

$$C = 1/(1 + aT\beta\eta) , \quad (21)$$

where a is a collection of previously described constants. By letting $\tau_R^0 = 0$ and absorbing additional constants into the coefficient b we can reduce Eq. (18) to

$$\eta/T\tau_R = b(1 + aT\beta\eta) . \quad (22)$$

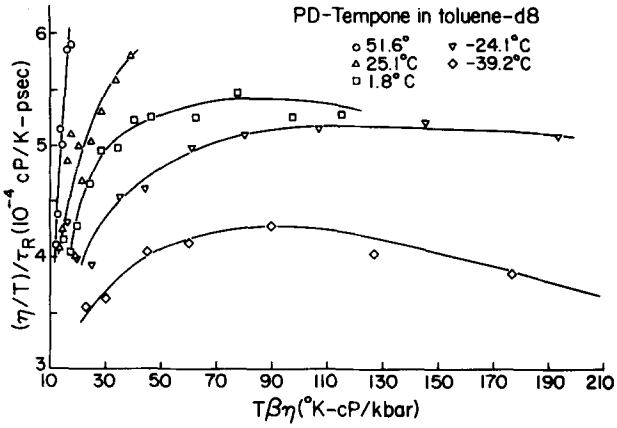

FIG. 8. Isotherms of η/τ_R vs $\beta\eta T$ for PD-Tempone in toluene-$d8$.

In Fig. 8 we have tested the functional form of Eq. (22) by plotting $\eta/\tau_R T$ vs $\beta\eta T$ as isotherms using the variable pressure data from Table I. The values of β we used are given in Table III.[34] Ideally the results for each isotherm should lie on the same straight line if Eq. (22) were exactly obeyed. Instead we find no such behavior. The isotherms are not linear nor do they approximate the same curve. These discrepancies are too large to be interpretable in terms of residual T and P dependence of a and b. We thus conclude that while the free-space model of Eqs. (18)–(20) has been useful in correlating a range of data on τ_R from different experiments, it is unsuccessful in dealing with the deviations from Stokes–Einstein behavior we observe in our present study [cf. Eqs. (16) or (17)].

We have examined a variety of functional relations in an effort to obtain further insight into these deviations. We believe we have found an empirical form that is successful in representing our observations. Our analysis leading to this expression is summarized in Table V. This table has been constructed in terms of constant density groupings (CDG), as is consistent with a free-volume or free-space point of view. We first note from this table that for each CDG the variation in $\beta\eta T$ is *opposite* to that trend required to explain the variation of $\beta\eta/T\tau_R$ with T according to Eq. (22), which derives from Kivelson's free-space model, (i.e., while $\eta/T\tau_R$ consistently decreases with decreasing T, $\beta\eta T$ increases and this increase is most dramatic at the higher densities). Next we find that $\eta\beta/T\tau_R$ is *constant* for each CDG within the experimental scatter; (i.e., we have cancelled out the systematic decrease with T of $\eta/T\tau_R$ for each CDG). In Fig. 9 we plot the mean values of $(\eta\beta/T\tau_R)^{-1}$ obtained for each CDG vs ρ, and we see these are nicely fit by a straight line. We then perform the more complete analysis of our pressure dependent data in Table V by subjecting all 48 entries in that table to a linear least-squares fit to

$$\tau_R T/\eta\beta = c(\rho - \tilde{\rho}) , \quad (23)$$

to obtain the slope c and intercept $c\tilde{\rho}$. We obtain $c = 25.6 \times 10^{-8}$ K s kbar-cm^3/g-cP. (Or $Nk_Bc = 51.5$ kcal/mol $\times$cm^3/g) and $\tilde{\rho} = 0.81$ g/cm^3 with an $R^2 = 0.90$ representing *as good* a fit to our data as the polynomial forms of

TABLE V. Constant density groupings and correlation of τ_R with thermodynamic and hydrodynamic properties.

ρ(g/cm^3)	T(K)	η(cP)	β(kbar^{-1})	$\tau_R\times10^{12}$(s)	$\frac{\eta}{T\tau_R}\times10^{-8}\frac{\text{cP}}{\text{K(s)}}$	$\beta\eta T\frac{\text{cP K}}{\text{kbar}}$	$\frac{\eta\beta}{T\tau_R}\times10^{-8}\frac{\text{cP}}{\text{K(s) kbar}}$
0.92	324.7	0.507	0.0778	3.65	4.28	12.8	0.333
0.94	324.7	0.607	0.0671	4.08	4.58	13.2	0.307
	298.2	0.647	0.0718	5.6	3.875	13.85	0.278
	Av						0.292 ± 0.021
0.96	324.7	0.731	0.0563	4.6	4.89	13.36	0.275
	298.2	0.784	0.0622	5.8	4.53	14.54	0.282
	274.9	0.896	0.0673	7.7	4.23	16.58	0.285
	Av						0.281 ± 0.005
0.98	324.7	0.887	0.0459	5.3	5.15	13.22	0.236
	298.2	0.969	0.0516	6.9	4.71	14.91	0.243
	274.9	1.092	0.0561	9.5	4.18	16.84	0.234
	249.0	1.332	0.0630	12.5	4.28	20.90	0.269
	Av						0.2455 ± 0.016
1.00	324.7	1.101	0.0380	6.25	5.42	13.58	0.206
	298.2	1.208	0.0411	8.3	4.88	14.81	0.201
	274.9	1.375	0.04606	11.8	4.24	17.41	0.195
	249.0	1.616	0.0508	15.3	4.24	20.44	0.215
	233.9	1.90	0.056	20.5	3.96	24.89	0.222
	Av						0.208 ± 0.011
1.02	324.7	1.410	0.0349	7.5	5.79	15.98	0.202
	298.2	1.542	0.0356	10.3	5.02	16.37	0.179
	274.9	1.798	0.0378	14.6	4.48	18.68	0.169
	249.0	2.007	0.0387	20.0	4.03	19.34	0.169
	233.9	2.286	0.0430	25.5	3.83	22.99	0.165
	Av						0.177 ± 0.015
1.04	324.7	1.80	0.030	9.4	5.89	17.53	0.177
	298.2	2.046	0.0331	13.1	5.24	20.19	0.173
	274.9	2.444	0.0333	18.5	4.904	22.37	0.160
	249.0	2.89	0.0350	27.4	4.23	25.19	0.148
	233.9	3.065	0.038	35.0	3.74	27.24	0.142
	Av						0.160 ± 0.015
1.06	298.2	2.610	0.029	17.2	5.09	22.57	0.148
	274.9	3.382	0.0331	24.0	5.125	30.77	0.170
	249.0	4.36	0.0355	37.8	4.63	38.54	0.164
	233.9	4.937	0.0356	50.8	4.15	41.11	0.147
	Av						0.157 ± 0.012
1.08	298.2	3.489	0.0255	22.5	5.20	26.53	0.133
	274.9	4.702	0.029	32.5	5.26	37.48	0.153
	249.0	6.70	0.0324	53.2	5.06	54.05	0.164
	233.9	7.744	0.0333	78.1	4.24	60.32	0.141
	Av						0.148 ± 0.014
1.10	298.2	4.981	0.0222	29.8	5.60	32.97	0.124
	274.9	6.076	0.0269	45.0	4.911	44.93	0.132
	249.0	10.16	0.0301	80.4	5.07	76.15	0.153
	233.9	12.92	0.0314	125.0	4.416	94.89	0.139
	Av						0.137 ± 0.012
1.12	298.2	7.367	0.0188	39.5	6.25	41.3	0.118
	274.9	9.293	0.025	64.2	5.26	63.87	0.132
	249.0	14.02	0.0286	110.0	5.12	99.84	0.146
	233.9	20.07	0.030	195.0	4.40	140.8	0.132
	Av						0.132 ± 0.012
1.14	274.9	14.49	0.0221	98.0	5.38	88.03	0.119
	249.0	21.12	0.0263	164.0	5.17	138.31	0.136
	233.9	27.8	0.0287	310.0	3.84	186.62	0.110
	Av						0.122 ± 0.013
1.16	274.9	21.80	0.0193	158.0	5.02	115.7	0.100
	249.0	32.9	0.024	250.0	5.28	196.6	0.127
	233.9	44.2	0.027	510.0	3.704	279.1	0.100
	Av						0.109 ± 0.016

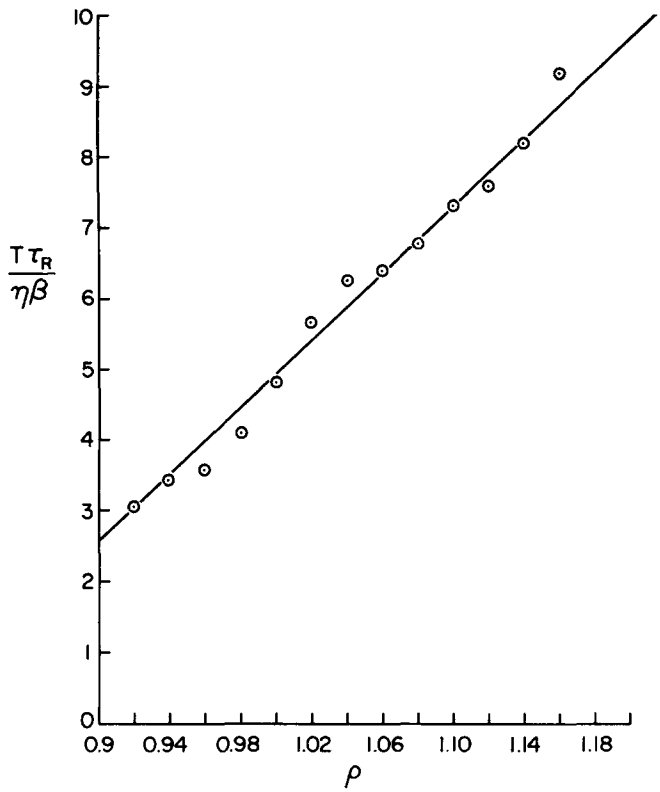

FIG. 9. Plot of average value of $\tau_R T/\eta\beta$ for each constant density group (CDG) vs density, ρ.

Eqs. (16) or (17) (even given the limited accuracy in estimating β from the PVT data of Table 3.2).[34] (A modified form where we let $c \to c'/\rho$, for which the statistical fit to our data is equally good, is discussed below.)

It is of interest to note that $\eta/T^2\tau_R$ is also found to be a constant for each CDG within experimental scatter. But when $T^2\tau_R/\eta$ is least-squares fitted vs ρ a decidedly poorer fit is obtained ($R^2 = 0.62$). We will examine below the reason for this.

D. Physical significance of empirical form for τ_R: Conjectures

We now raise the question of the physical significance of the empirical form given by Eq. (23). We first address the question of the uniqueness of this fit. We cannot claim to have attempted all conceivable possibilities, so one must leave open the possibility that some other physical parameter(s) with the same functional dependence (on T and ρ) as $\beta(\rho - \tilde{\rho})$ could be acceptable. In particular, it would be better for purposes of interpretation if c were dimensionless. {In this spirit we suggest below that if we replace β by αT, [cf. Eq. (13a) for α] which is dimensionless, it might be possible to achieve a modification of Eq. (23) in terms of dimensionless parameters.}

If β (or αT) is truly involved in the functional dependence as expressed in Eq. (23) it would follow that the compressibility of the solvent is playing a significant role in the molecular reorientational dynamics. The Stokes–Einstein model is, of course, valid for an incompressible fluid. Our result would then be somewhat at odds with the theoretical observation of Masters and Madden[6] who suggest from their generalized hydrodynamic analysis that compressibility effects are likely to be less important for a rotating molecule than a translating one.

Let us, then, attempt to examine Eq. (23) in terms of a simple physical model, which does not necessarily depend on the resolution of the compressibility question. Here we use the simple free-volume point of view of Frenkel[32] (see also Ref. 3). In the free volume theory we rewrite β as

$$\beta = \frac{V_f}{V_0}\frac{\Delta v}{k_B T}, \tag{24}$$

where $V_f = V - V_0$ is the free volume of the liquid, and V_0 is the smallest volume (i.e., close-packed volume) of the liquid. [We follow Frenkel who has let $V \approx V_0$ in the denominator of Eq. (24).] Also Δv represents the smallest volume of a hole (per solvent molecule). We have examined the validity of Eq. (24) for toluene-$d8$. Indeed we find that βT is reasonably constant for each CDG (cf. Table V). We have plotted the mean value of βT for each CDG vs ρ^{-1} in Fig. 10. This form is suggested by $(V - V_0) = (\rho_0/\rho) - 1$, where $V_0^{-1} \equiv \rho_0$. Thus, a linear plot is expected from Eq. (24) with ρ_0^{-1} the intercept of the ρ^{-1} axis and $\rho_0 \Delta v/k_B$ the slope. Instead, we find two regions: a low and a high density region,

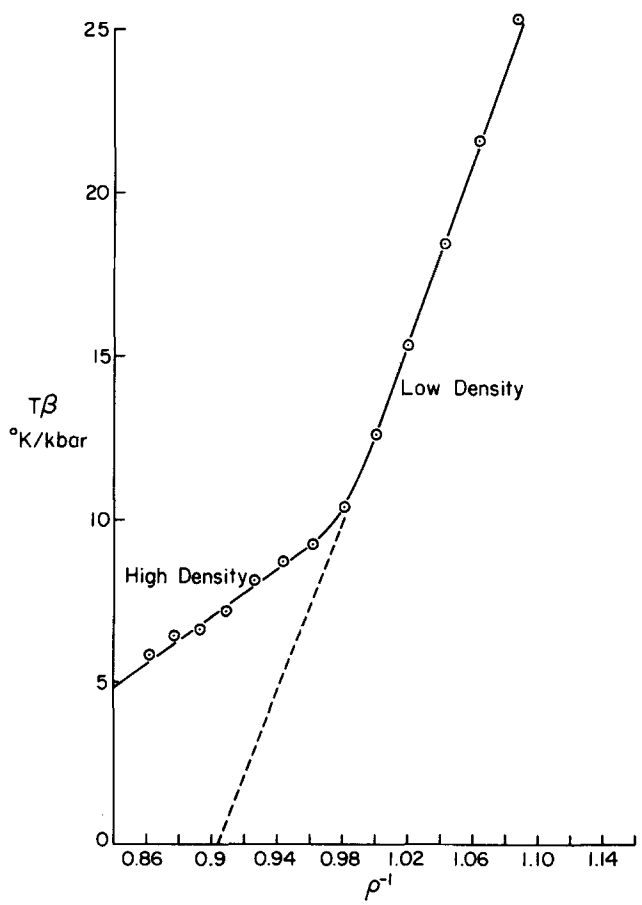

FIG. 10. Plot of average value of βT for each constant density group (CDG) vs inverse density, ρ^{-1}.

each of which show good linear behavior. This is to be expected; Frenkel points out that β should be the sum of two parts. At high density there is just a *geometrical* part in which the dimensions of a regular packed structure decrease with applied pressure; while at low density there is an additional *structural* contribution to β, as the applied pressure tends to impose the regular structure on the more random arrangements of molecules. In particular, we find $\rho_0 \approx 1.1$ and 1.4 g/cm^3 for the low and high density lines, respectively, while $N\Delta v \approx 9.9$ and 3.2 cm^3/mol, respectively. Thus the "hole size" Δv is substantially larger in the low density more random fluid, and the free volume of the low density fluid is referred to a more open and less dense structure. [We note in passing that Δv for the low density fluid is of the order of Δv_a in Fig. 4(b).]

It is now clear why the function $\eta/T^2\tau_R$ was found to be constant for each CDG, yet did not lead to a satisfactory fit to the data. The two-region shape of βT vs ρ^{-1} of Fig. 10 was required to correlate our results on τ_R!

We now introduce the more questionable Batchinski equation for η[3,32,33]:

$$\eta^{-1} \approx B(V_f/V_0)\,, \tag{25}$$

where B should be a constant for each system. When we plot η^{-1} vs ρ^{-1} as suggested by Eq. (25), we find a family of straight lines lying close to each other for the isotherms; i.e., $B = B(T)$, and for $\rho^{-1} \lesssim 0.92$ these lines bend to become new lines of smaller slope by analogy to βT in Fig. 10. The high density η^{-1} lines go to zero at a lower density ($\rho_0 \approx 1.2$ g/cm^3) than βT. We will ignore this non-negligible dependence of B on T and ρ for the present qualitative argument. It is well known that the Batchinski relation is not adequate for quantitatively representing viscosities [cf. Eq. (4)], [15] but it has some qualitative value in exploring models.

Then, if we modify Eq. (23) (which is the simplest form that fits the data) to

$$\tau_R T/\eta\beta = c'(\rho - \tilde{\rho})/\rho \tag{23'}$$

[for which a least-squares analysis yields $c' = 31.9\times10^{-8}$ K s kbar/cP and $\rho = 0.845$ g/cm^3 with about as good a statistical fit as Eq. (23)], we obtain using Eqs. (24) and (25):

$$\tau_R = \frac{c'\eta\beta}{T}\left(\frac{\tilde{V}-V}{\tilde{V}}\right) \approx \frac{c'}{B}\,\frac{\Delta v}{k_B T^2}\left(\frac{\tilde{V}-V}{V}\right), \tag{26}$$

(where $\tilde{V} \equiv \tilde{\rho}^{-1}$), which we refer to as an *expanded-volume* model versus the free-volume-Stokes–Einstein form obtained by inserting Eq. (25) into Eq. (1):

$$\tau_R \approx \frac{v_p}{k_B T B}\left(\frac{V_0}{V-V_0}\right). \tag{27}$$

Thus, the most important change is seen to be the replacement of $\tau_R \propto V_f^{-1}$ by a $\tau_R \propto \Delta V_e \equiv \tilde{V} - V$ for the expanded volume model. These are physically different results. The Stokes–Einstein-free-volume result implies that $\tau_R \to \infty$ as $V \to V_0$ corresponding to the dense close-packed limit with no free volume, which is the reference state. One can still have rotation for dense packing with slip boundary conditions on a nearly spherical molcule, so one often modifies the Stokes–Einstein equation (1) by multiplying by $f_{\text{slip}} < 1$ to allow for slip in attempting to fit experimental data.[2] Our relation giving $\tau_R \propto \tilde{V} - V$ compares the actual specific volume with an *expanded volume* $\tilde{V}$. As V expands toward $\tilde{V}$, the free space in which the molecule can rotate is increasing, so the anisotropic forces on the molecule are reduced, and it is freer to rotate. In the limit $V \to \tilde{V}$ the liquid has expanded so much that the molecule is completely free to rotate, i.e., this is the limit of perfect slip. This is an artificial limit in the sense that the range of τ_R we have studied corresponds to pure viscous motion.[1] Before the limit $V \to \tilde{V}$ is reached, the volume has expanded sufficiently that inertial effects become important in the reorientational dynamics, so the description of τ_R should change in a natural manner over to an inertial form. Thus $\tilde{V}$ is a reference volume such that $\tau_R \to 0$ as $V \to \tilde{V}$ *if inertia could be neglected.* The main point is that ΔV_e is a measure of the strength of the anisotropic intermolecular interactions acting on the rotating molecule in such a way as to naturally incorporate the concept of slip. [The other limit as $\Delta V_e \to \tilde{V} - V_0$ would seem to lead to a constant finite value of τ_R, but we should remember that Eqs. (24) and (25) are not exact, and the quantity $\eta\beta T \to \infty$ as $T \to 0$, (cf. Table V) because $\eta^{-1} \to 0$ at a lower density than $\beta T \to 0$, (cf. above). Thus τ_R can still increase in the high density regime.]

Before leaving the free-volume point of view, we offer some further conjectures. We first note that in the free-volume theory, the dimensionless $\alpha T = \beta(U/\Delta v)$, where U is an activation energy defined by $V_f = N\Delta V \times \exp(-U/kT)$.[32] Let us use this expression to rewrite Eq. (23') in terms of *dimensionless* parameters as

$$\left(\tau_R \frac{kT}{v_p \eta}\right) = a(\alpha T)\left(\frac{\tilde{V}-V}{\tilde{V}}\right), \tag{28}$$

where a is dimensionless and we shall assume nearly constant (a matter to be checked in future work). Using the free-volume form of αT and comparing Eq. (28) to Eq. (23'), we get $a \approx (kc')\Delta v/v_p U$. Of course, Δv has two values and U is not known, so let us use Eq. (12) which yields $\alpha T = \beta(\Delta H_a - \Delta E_a)/\Delta V_a$ to obtain $a \sim 4$ (but not exactly constant). Equation (28) is clearly speculative, but before leaving it, we use it to consider the approach to a Stokes–Einstein limit: This would occur when $\tilde{V}/V \to \infty$, i.e., when the Brownian particle becomes so large (of radius r_B) that $\tilde{V} \sim \frac{4}{3}\pi r_B^3 \gg V$. This suggests we regard $\tilde{V} = \tilde{V}(v_p/v_s)$, where v_s is the volume of a solvent molecule, and $\tilde{V}$ probably also depends on the shape (i.e., deviation from sphericity) of the probe molecule. We also would require $a\alpha T$ to be replaced by some function, which approaches unity as β (or α) becomes small enough (e.g., $1 + a\alpha T$ is of order unity for our results).

It is difficult, at present to connect Eq. (23) with more fundamental molecular theory, and that is why the above discussion in terms of free volume ideas was used. However, a few comments in relation to molecular theories might be in order. The point of view that we find most amenable is due to Kivelson.[35] In this molecular point of view the dimensionless factor C of Eq. (18), (also referred to as κ, as pointed out the

previous section) depends upon

$$\kappa \propto \langle \mathcal{T}\mathcal{T} \rangle / \langle \sigma\sigma \rangle , \tag{29}$$

i.e., the ratio of the equilibrium correlation function of the torques $\mathcal{T}$ over that for the stress tensor σ. That is, since η, the shear viscosity, is associated with translational motion, then κ is a "coupling parameter" relating to translational effects, and it appears in Eq. (29) as "the ratio of torques to forces or anisotropic intermolecular interactions to total intermolecular interactions". Now our empirical equation (23) or (28) suggests we write

$$\kappa \propto \beta \left(\frac{\Delta V_e}{V}\right) \propto \left(\frac{\Delta V_e}{V}\right)/c^2 , \tag{30}$$

where c the velocity of sound is given by[36] $c^2 = (c_p/c_v)(\beta\rho)^{-1}$ [and we are assuming in the second form of Eq. (30) that the variation in c^2 with T and ρ far from the critical point is dominated by its inverse dependence upon β]. We can regard c^2 as a measure of the total intermolecular interactions, while ΔV_e is a measure of the anisotropic intermolecular interactions acting on the probe molecule (as discussed above). Thus, our empirical equation (23) is in the spirit of Eq. (29)!

E. Comparison with other studies

We come now to a comparison with the results of other pressure-dependent studies. Fury and Jonas[28] report that in their NMR studies of neat liquids they find κ to decrease significantly with ρ, and with a weaker dependence on T but increasing with T. This behavior is true for toluene-$d8$.[12] It follows from Eq. (17) that we find the same density dependence for PD-Tempone in toluene-$d8$, but, in the temperature range studied, we obtain the opposite temperature dependence.

We have found some evidence for a similar trend with T (i.e., a decrease in κ with increasing T) in the experiments with PD-Tempone in other solvents reported in I[1] at atmospheric pressure from a comparison of the respective temperature-dependent activation energies for τ_R and for η/T. These effects were small enough that they did not hinder obtaining good linear τ_R vs η/T plots within experimental error. Our present study on PD-Tempone in toluene-$d8$ has enhanced such incipient deviations by working at higher pressure [cf. Eq. (16) and discussion below].

Hwang *et al.*[11] in their ESR studies of VOAA in toluene and other solvents find that κ is independent of T, P, (and ρ) and depends only on solvent. In comparing their results to the work of Jonas *et al.*, they point out that the latter studied systems where the solvent and solute were identical, whereas for VOAA, the solvent molecules were small compared to the solute molecules, which favors rotational diffusion, and furthermore the molecules studied by Jonas exhibit inertial effects. We believe that our results of PD-Tempone in toluene are an intermediate case. PD-Tempone is a little larger than toluene-$d8$ (e.g., a molecular weight of 186 versus 100), and of somewhat different shape (i.e., more of an ellipsoid) than the more disklike toluene. Also, the nitroxide group probably interacts to a small extent with the aromatic ring of the toluene (cf. the E_T scale in I). Thus, for reasons of size and shape, as well as the regions of T and ρ studied, inertial effects should be negligible in our results, as in those on VOAA. This may account for the different T dependence of κ between our results and those of Jonas. On the other hand PD-Tempone is not so large as to have approached the Brownian motion limit. The fact that $\epsilon > 1$ for PD-Tempone in toluene[8] (and a variety of solvents, cf. I), while VOAA in toluene (and other solvents) yields $\epsilon \sim 1$ consistent with a Debye spectral density appropriate for Brownian reorientation,[37] is supportive of this.[38] Further support comes from the slow-motional ESR lineshape analyses, which show that VOAA in toluene is well described by a Brownian reorientational model,[37] while PD-Tempone in toluene is well described by a moderate-jump model.[8]

TABLE VI. Comparison of activation energies and activation volumes.

ΔH_a[b]	P(kbar)	ESR	η/T[a]	NMR[a]
kcal/mol	1	2.95	2.55	1.79
	1.5	3.66	3.02	2.35
	3	4.72	3.56	2.56
ΔE_a[c]	ρ(g/cm^3)			
kcal/mol	0.96	1.85	1.31	0.86
	1.00	1.90	1.34	1.05
	1.04	2.17	1.51	1.30
ΔV_a[d]	t°C		η	
cm^3/mol	−35	13.5	14.8	11.4
	0	12.2	14.1	10.7
	50	10.3	14.9	9.9

[a]From Wilbur and Jonas (Ref. 12).
[b]ESR results from Eq. (7).
[c]ESR results from Eq. (9).
[d]ESR results from Eq. (11).

Additional evidence to support our belief that our results on PD-Tempone in toluene-$d8$ represent a different region in which inertial effects are unimportant, versus the results of Wilbur and Jonas on neat toluene-$d8$ comes from the measured activation energies and volume. This is summarized in Table VI. Wilbur and Jonas found that the activation energies and volume for reorientation of toluene-$d8$ were consistently *smaller* than those for the viscosity. This was interpreted in terms of weaker rotational-translational coupling, that may permit more inertial character to the rotational motion. (This argument is supported by the even lower activation values for the internal rotation of the methyl ring, which should be even more inertial.) Our observed ΔV_a for PD-Tempone are more nearly equal to those for η, especially at the lower temperatures [but recall that ΔV_a^{η} appears to have some pressure dependence cf. Fig. 4(b)]. Our ΔH_a and ΔE_a are systematically *larger* than those for the viscosity. This suggests to us strong coupling to the viscous modes but with additional specific interaction between solute and solvent molecules as we have already inferred.

When Fury and Jonas[28] reanalyzed their results on κ utilizing Eq. (14) above, (we presume by the approach of Table II), they found κ independent of density, (but unlike their statement that κ is independent of T within experimental error, we find for the data of Wilbur and Jonas[12] that κ/T is more nearly constant). We have already concluded from our analyses summarized in Tables II, III, and IV, that Eq. (14) is not a satisfactory method to analyze our results. The same is likely true for the other studies. Even if those studies are complicated by inertial contributions, our understanding of the way such contributions affect τ_R,[39,40] shows us that there should be nonlinear curvature in plots of τ_R vs η/T, provided a sufficient range of τ_R is studied!. Our own anomalous linear fits of τ_R vs η/T summarized in Tables II, III, and IV were reinterpreted by Eq. (16) or (17) as a consequence of each such line covering a sufficiently small region of a general nonlinear curve that it is approximately linear but the slope and intercept will not be the same. (In our case, as we have said already, the anomalies are not attributable to inertial effects.)

We now wish to make a few comments about the studies of PD-Tempone as a function of temperature at atmospheric pressure for different solvents.[1,8] First let us consider toluene solvent. Equation (16) predicts only a small variation in $\tau_R T/\eta$ with T for $P=1$ bar, e.g., from 80 °C to −40 °C it increases by 10%, an amount that could be obscured by experimental uncertainties. However, for $P=3$ kbar, over the same temperature range it increases by 35%, clearly a more significant amount. Thus the effects we observe are more pronounced at the higher pressures. Furthermore, the variations in $\tau_R T/\eta$ with *two* independent thermodynamic variables, in particular, T and ρ allowed us the opportunity to isolate specific trends, and this is no longer possible from only temperature-dependent studies. With these provisos in mind we did examine the possible applicability of Eq. (23) to the solvent-dependent data. This was further hampered by inadequate data on β for most of the solvents, especially at the lower temperatures where $\tau_R T/\eta$ appears to show larger variation. Nevertheless, we did, in general, find Eq. (23) useful as an empirical function in fitting the limited range of data to the two parameters C and $\tilde{\rho}$ in place of the more conventional A and τ_R^0 of Eq. (14), although with not quite as good statistics.[41] A fit to Eq. (23) could even be found in cases where $\tau_R T/\eta$ hardly varied over the limited range of T for which adequate data (on e.g., β) was available (e.g., n-decane and acetone). We regard this as merely a demonstration that Eq. (23) is reasonably consistent with much of this data even though results as a function of only T (especially over only limited ranges of T) are usually too insensitive to provide a critical test. We may expect that as more solvents and other systems are studied as a function of both T and P, improved versions of Eq. (23) may be found, especially since our present study emphasized a small range of $\rho-\tilde{\rho}$.

Thus, we conclude that our empirical Eq. (23) or (23′) and the related speculative interpretations should be regarded as appropriate for the case of a solute in a solvent of somewhat smaller molecular size and with a specific, though not very strong, solute–solvent interaction. Furthermore, it requires inertial effects to be unimportant. It remains to be seen how this or other empirical forms can be extended to other cases.

IV. CONCLUSIONS

(1). Our extensive data for $\tau_R(T,P)$ covering more than two orders of magnitude in τ_R could not be consistently interpreted in terms of a simple η/T behavior with nonzero intercept.

(2). A successful empirical fit of form $\tau_R = c\eta\beta(\rho-\tilde{\rho})/T$ was found.

(3). This fit is suggestive of an "expanded volume" model for rotational reorientation, in which τ_R is proportional to the deviation of the specific volume of the liquid from a larger reference volume, the expanded volume, and this deviation is a measure of the anisotropic intermolecular interactions acting on the probe.

(4). A comparison of these results on a solute of molecular size somewhat greater than that of the solvent molecules with NMR results on neat liquids suggests some differences in their respective behavior, which could be due to the direct importance of inertial effects in the latter.

(5). The extensive results for PD-Tempone in toluene-$d8$ as a function of T and P show that the rotational reorientation is isotropic independent of T and P and also the ϵ correction to the nonsecular spectral densities is independent of T and P for $\tau \gtrsim 5$ ps. The latter appears reasonably consistent with the fluctuating torque mechanism previously postulated by Hwang, Mason, Hwang, and Freed.

[1]S. A. Zager and J. H. Freed, J. Chem. Phys. 77, 3344 (1982).
[2]D. Kivelson and P. A. Madden, Annu. Rev. Phys. Chem. 31, 523 (1980).
[3]J. L. Dote, D. Kivelson, and R. N. Schwartz, J. Phys. Chem. 85, 2169 (1981).
[4]W. A. Steele, Adv. Chem. Phys. 34, 1 (1976).
[5]J. T. Hynes, R. Kapral, and M. Weinberg, J. Chem. Phys. 69, 2725 (1978).
[6]A. J. Masters and P. A. Madden, J. Chem. Phys. 74, 2450 (1981).
[7]S. A. Goldman, G. V. Bruno, C. F. Polnaszek, and J. H. Freed, J. Chem. Phys. 56, 716 (1972); S. A. Goldman, G. V. Bruno, and J. H. Freed, *ibid.* 59, 3071 (1973).
[8]J. S. Hwang, R. P. Mason, L. P. Hwang, and J. H. Freed, J. Phys. Chem. 79, 489 (1975).
[9]J. Jonas, Annu. Rev. Phys. Chem. 26, 167 (1975); Adv. Magn. Reson. 6, 73 (1973).
[10]J. S. Hwang, D. Kivelson, and W. Z. Plachy, J. Chem. Phys. 58, 1753 (1973).
[11]J. S. Hwang, K. V. S. Rao, and J. H. Freed, J. Phys. Chem. 80, 1490 (1976).
[12]D. J. Wilbur and J. Jonas, J. Chem. Phys. 62, 2800 (1975).
[13]S. A. Zager, Ph.D. thesis, Cornell University, 1981.
[14]W. Z. Plachy, Ph.D. thesis, University of California, Los Angeles, California, 1967.
[15]A. J. Barlow, J. Lamb, and A. J. Matheson, Proc. R. Soc. London Ser. A 292,322 (1966).
[16]L. Bosio, A. Defrain, and G. Folcher, J. Chim. Phys. 73,

913 (1976); J. Osugi, K. Shimizu, and A. Onodera, Rev. Phys. Chem. Jpn. 34, 97 (1964).
[17]J. F. Skinner, E. L. Cussler, and R. M. Fuoss, J. Phys. Chem. 72, 1057 (1968); E. B. Freyer, J. C. Hubbard, and D. H. Andrews, J. Am. Chem. Soc. 51, 759 (1929); R. I. Mopsik, J. Chem. Phys. 50, 2559 (1969).
[18]P. W. Bridgman, Proc. Am. Acad. Sci. 61, 57 (1926).
[19]H. J. Parkhurst, Y. Lee, and J. Jonas, J. Chem. Phys. 55, 1368 (1971).
[20]R. G. Parker and J. Jonas, J. Magn. Reson. 6, 106 (1972).
[21]J. G. Powles and M. C. Gough, Mol. Phys. 16, 349 (1969).
[22]R. L. Armstrong and P. A. Speight, J. Magn. Reson. 2, 141 (1970).
[23]We further note that the present work is consistent with the activated state analyses resulting from variable pressure and temperature studies of other systems. For molecular liquids, these include treatment of nuclear spin lattice relaxation times for several normal hydrocarbons and the isomers of hexane [D. W. McCall, D. C. Douglass, and E. W. Anderson, Phys. Fluids 2, 87 (1959)], normal heptane [J. G. Powles and M. C. Gough, Mol. Phys. 16, 349 (1969)] deuterated chloroform [D. L. VanderHart, J. Chem. Phys. 60, 1858 (1974)], and deuterated glycerol [M. Wolfe and J. Jonas, J. Chem. Phys. 71, 3252 (1979)]. A related ESR relaxation study of PD-Tempone in the nematic liquid crystal Phase V [J. S. Hwang, K. V. S. Rao, and J. H. Freed, J. Phys. Chem. 80, 1490 (1976); W. J. Lin and J. H. Freed (to be published)] has been discussed in terms of the activated state parameters. Also within this framework, molecular rotation in simple crystalline solids has been considered using methods such as nuclear spin lattice relaxation [J. E. Anderson and W. P. Slichter, J. Chem. Phys. 44, 1797 (1966); R. Folland, S. M. Ross, and J. H. Strange, Mol. Phys. 26, 27 (1973); S. M. Ross and J. H. Strange, J. C Chem. Phys. 68, 3078 (1978)] and nuclear quadrupole resonance [M. Oron, A. Zussman, and E. Rapoport, J. Chem. Phys. 68, 794 (1978)].
[24]D. R. Bauer, J. I. Brauman, and R. Pecora, J. Am. Chem. Soc. 96, 6840 (1974).
[25]G. R. Alms, D. R. Bauer, J. I. Brauman, and R. Pecora, J. Chem. Phys. 58, 5570 (1973); 59, 5310 (1973).
[26]S. Claesson and D. R. Jones, Chem. Scr. 9, 103 (1976).
[27]F. G. Herring and J. M. Park, J. Magn. Reson. 36, 311 (1979); F. G. Herring and P. S. Phillips, J. Chem. Phys. 73, 2603 (1980).
[28]M. Fury and J. Jonas, J. Chem. Phys. 65, 2206 (1976).
[29](a) In I we found that τ_R vs η/T obtained by varying T for different solvents (instead of different pressures) also yielded a variety of different results for τ_R^0 ranging from non-negligible positive values (e.g., decane and dodecane solvent) to zero values (e.g., D_2O and DNBPT) to significant negative values (e.g., acetone, ethanol, and glycerol). Our discussion given for this matter with respect to the pressure studies may be applicable to these solvent dependent effects as well; (b) this analysis required extensive interpolation from Table I; analytical and graphical methods were checked for consistency. It is important to obtain accurate interpolations because each isochore is not only shorter than any isotherm or isobar but contains fewer data points as well.
[30]SAS, *Statistical Analysis Systems Users Guide*, edited by J. T. Helwig and K. A. Council (SAS Institute, Raleigh, N.C., 1979).
[31]C. Daniel and F. S. Wood, *Fitting Equations to Data Computer Analysis of Multifactor Data for Scientists and Engineers* (Wiley, New York, 1971).
[32]J. Frenkel, *Kinetic Theory of Liquids* (Dover, New York, 1955).
[33]J. H. Hildebrand, Science 174, 490 (1971).
[34]These values of β were first smoothed by least-squares fitting the finite difference values to the linearized form of the Tait equation [cf. J. F. Skinner, E. L. Cussler, and R. M. Fuoss, J. Phys. Chem. 72, 1057 (1968)].
[35](a) D. Kivelson, M. G. Kivelson, and I. Oppenheim, J. Chem. Phys. 52, 1810 (1970); (b) D. Kivelson, Chem. Soc. Faraday Symp. 11, 7 (1977).
[36]L. Landau and L. Lifshitz, *Fluid Mechanics* (Pergamon, London, 1959), p. 247.
[37]R. F. Campbell and J. H. Freed, J. Phys. Chem. 84, 2668 (1980).
[38]It is difficult to study the ϵ correction of Eq. (2) by NMR, because the lower frequencies lead to the extreme narrowing condition for liquids. B. Blicharska, H. G. Hertz, and H. Versmold, [J. Mag. Res. 33, 531 (1980)] have succeeded in a study of CH_3OH in $(CD_3)_2SO$ to reach the $\omega\tau_R \approx 1$ regime. The anomalies they see are consistent with an $\epsilon > 1$ possibly from a fluctuating torque model (cf. Ref. 1).
[39]P. S. Hubbard, Phys. Rev. A 6, 2421 (1972); 8, 1429 (1973); 9, 481 (1974).
[40]G. V. Bruno and J. H. Freed, J. Phys. Chem. 78, 935 (1974).
[41]Some results of fits to Eq. (23) for C and $\tilde{\rho}$ (in units of K skbar cm^3/g cP and g/cm^3, respectively) were 3.0×10^{-7} and 0.63 for acetone ($r^2 = 0.90$ using PVT data for the undeuterated case); 2.0×10^{-7} and 0.61 for ethanol ($r^2 = 0.90$ using PVT data for the undeuterated case); 1.9×10^{-7} and 0.65 for n-decane; 2.5×10^{-8} and 0.94 for CCl_4, the highest density liquid. From the limited data on DNBPT both $\tilde{\rho}$ and β appear nearly constant, while β for D_2O exhibits unusual behavior, passing through a broad minimum. The results for acetone, ethanol and n-decane compare favorably with the results of 2.56×10^{-7} and 0.81 reported above for the somewhat denser toluene-$d8$.